Journal of Atmospheric and Solar-Terrestrial Physics 138-139 (2016) 161–168

Contents lists available at ScienceDirect

Journal of Atmospheric and Solar-Terrestrial Physics

journal homepage: www.elsevier.com/locate/jastp

Research Paper

Long-term variation of OH peak emission altitude and volume emission rate over Indian low latitudes

M. Sivakandan [a], T.K. Ramkumar [a], A. Taori [a,*,1], Venkateshwara Rao [b], K. Niranjan [c]

[a] National Atmospheric Research Laboratory, Gadanki 517112, India
[b] Government College (Autonomous), Rajahmundry 533105, India
[c] Department of Physics, Andhra University, Visakhapatnam 530003, India

ARTICLE INFO

Article history:
Received 8 June 2015
Received in revised form
5 January 2016
Accepted 14 January 2016
Available online 15 January 2016

Keywords:
Mesospheric OH airglow
Solar influence
AO-SAO-QBO-ENSO signatures
SABER and ECMWF data

ABSTRACT

Using 13 (April 2002–December 2014) years of Sounding of the Atmosphere using Broadband Emission Radiometry (SABER/TIMED) 1.6 μm OH airglow emission data, we have studied the long-term variation of OH peak emission altitude and volume emission rate (VER) for 0–10°N latitude and 70–90°E longitude grid. We have noted that, during day time the OH peak emission altitude is varying from 80 to 87 km with mean value of 83.5 km and from 82 to 88 km with mean value of 85 km during night time. The signature of semi-annual oscillation (SAO), annual oscillation (AO) and quasi-biennial oscillation (QBO) in the OH peak emission altitude as well as the VER is evident. Our analysis reveals that the SAO and QBO signatures but not the AO signature are very strong in the equatorial region during night time. Apart from the SAO, AO and QBO signatures, the presence of oscillation related to the El Niño oscillation (ENSO) is also noted. After the removal of these oscillations, we find the evidence of the influence of solar activity and a long term trend in the OH emission layer. It is also found good correlation between the mesospheric and stratospheric variations (ECMWF data).

1. Introduction

Hydroxyl (OH) airglow emission is the most intense emission occurring in the earth's upper atmosphere. Since the discovery of this emission by Meinel (1950), OH airglow emissions have been utilized to study the mesospheric processes (e.g., Khomich et al. (2008), Taori et al. (2005, 2012) and references cited therein). The prominent emission mechanism of the OH night airglow emission is the reaction between odd Hydrogen and Ozone (Meriwether, 1989; Xu et al., 2012),

$$O_3 + H \rightarrow OH(\vartheta \le 9) + O_2 + 3.3\text{eV} \quad (1)$$

Together with the above reaction, there is significant contribution from per-hydroxyl (HO_2) radicals reacting with oxygen as follows (Xu et al., 2012).

$$HO_2 + O \rightarrow OH(\vartheta \le 6) + O_2 \quad (2)$$

During daytime, apart from the above mentioned mechanisms water vapor-Herzberg continuum ($H_2O + h\nu(\lambda < 242\text{ nm}) \rightarrow OH(X^2\Pi) + H$) and water vapor – Lyman alpha line ($H_2O + h\nu(\lambda = 121.6\text{ nm}) \rightarrow OH(X^2\Pi) + H$) reactions also contribute to the observed OH emission (e.g., Khomich et al., 2008).

Owing to their large life time compared to the inter-collision time, the OH Meinel band emissions have been widely used for understanding the dynamical features occurring at the mesospheric altitudes (e.g., Meriweather (1984), Takahashi et al. (1995), Greet et al. (1997)). The OH night airglow emissions have also been extensively used to study the mesospheric wave and tidal features (Yee, 1991; Zhang and Shepherd, 1999; Zhang et al., 2001; Taori et al., 2005, 2007). For example, using scanning spectrometer, by monitoring OH (6,2) emission Takahashi et al. (1999) identified gravity waves with intrinsic periods of 2–9 h and horizontal wavelengths of 500–3000 km over Shigaraki, Japan. Further, using OH(6,2) and O_2 mesospheric temperature data, Taylor et al. (2005) studied the characteristics of the mesospheric semi-annual oscillation (SAO) over Maui, Hawaii. In the same line, variation of OH emission intensity exhibiting SAO features is reported by several investigators worldwide (e.g., Takahashi et al. (1995); Buriti et al. (2004), Taori et al. (2012)).

There have been few space borne probes to study the OH emission variability. Using Wind Image Interferometer (WINDII) onboard the Upper Atmospheric Research Satellite (UARS), Zaragoza et al. (2001) showed that SAO variations are stronger over low latitudes and that the AO signatures are dominent in

* Corresponding author.
E-mail address: alok.taori@gmail.com (A. Taori).
[1] Present address: National Remote Sensing Center (NRSC), Hyderabad 500037, India

http://dx.doi.org/10.1016/j.jastp.2016.01.012
1364-6826/

midlatitudes. Further, Shepherd et al. (2006) reported the distinct mesospheric semi-annual oscillation (MSAO) and Quasi-biennial oscillation (QBO) modulation over the equatorial and low latitudes. Like that, using 7 years of WINDII data, Liu et al. (2008) reported the climatology of seasonal variation of night time OH emission rate at mid-to-high latitudes. Recently, using 7 years of Sounding of the Atmosphere using Broadband Emission Radiometry (SABER) instrument on board the Thermosphere Ionosphere Mesosphere Energetics and Dynamics (TIMED) satellite, Gao et al. (2010) studied the global distribution of SAO, AO and QBO. They also noted that the emission intensity in the southern hemisphere is weaker than in the northern hemisphere.

As an extension of the above, in the present study, we investigate the characteristics of long term (annual, semi annual, quasi-biennial, ENSO) variation of the OH peak emission rate as well as the peak emission altitude over the Indian low latitudes. For this purpose, we used 13 years (2002–2014) of SABER satellite data averaged within the Indian tropical region of 0–10°N latitude and 70–90°E longitude. Apart from the oscillations investigated by Gao et al. (2010), we have investigated also other evident features in data such as the signatures of solar flux variations and residual trends.

2. Data set and methodology

2.1. SABER satellite data

Remote sensing the atmosphere at 10 different channels covering the wavelengths of from 1.27 μm to 17 μm, the SABER instrument onboard the TIMED satellite provides information about the middle atmospheric temperature, pressure, density, trace gases like ozone, CO_2 and OH airglow emission rates with 2 km altitude resolution (Remsberg et al., 2008). Among these 10 channels, two channels are dedicated for the measurement of mesospheric OH airglow emissions. Out of these two channels, while the channel A measures the OH emission at 2.0 μm which has contributions from the OH (9–7) and OH(8–6) vibrational transitions the channel B measures the OH emission at 1.6 μm which has contributions from the OH (5–3) and OH (4–2) vibrational transitions. Channel A represents transitions between higher vibrational levels ($\upsilon \geq 6$) while Channel B represents transitions between lower vibrational levels ($\upsilon \leq 6$) (Gao et al., 2010). In the present study, we use the data of OH emission at 1.6 μm.

For the Indian region low-latitude OH emission variability, we selected the geographical grid comprising of latitude 0–10°N and longitude 70–90°E within which the data are averaged and constructed the height profiles of OH emission, temperature and O_3 volume mixing ratio. Separate day time (0600–1800 h local time) and night time (1800–0600 h local time) profiles are considered to study the long term variations. Fig. 1 shows the day time (top panel) averaged OH emission profile on 20 June 2005 for the above mentioned latitude and longitude grid. In this figure, L_s indicates the layer stating point, L_e the end point and L_p the height of peak emission rate. In order to understand long-term variations in the OH emission, we have taken only the peak emission rate (PER) and its corresponding altitude. The bottom panel of this Fig. 1 is for a night time profile. It may be noted that the day and night time x-axis scales are different as the night time OH emission rate is 8–10 times greater than the day time emission rate (Gao et al., 2015). This analysis has been performed for each day (day and night separately) of all the years from 2002 to 2014.

2.2. Solar flux data

The measured daily solar flux (F10.7cm) data are obtained from the Canadian Space Weather website (http://www.spaceweather.gc.ca/solarflux/sx-5-mavg-en.php). Each measurement of the F10.7cm solar flux is expressed in three values: the observed, adjusted and URSI Series D (absolute) values. Here, we used annual average of observed values as well as the absolute solar flux values.

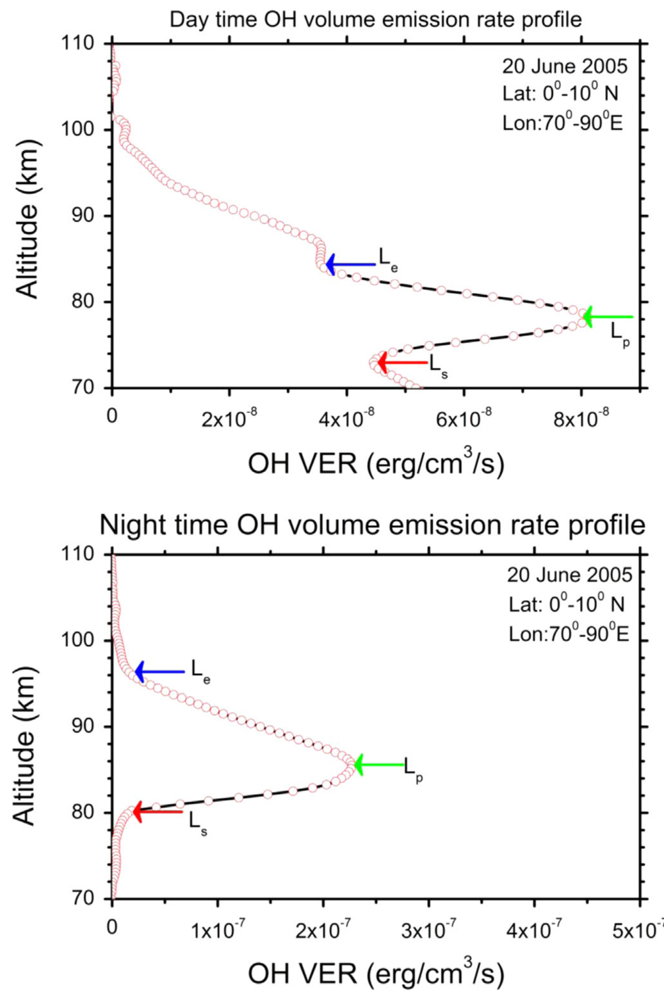

Fig. 1. Top panel show a sample of day time SABER OH volume emission rate profile (on 20 June 2005) for 0–10°N latitude and 70–90°E longitude grid. In this L_s and L_e are the starting and end point of the peak emission layer and L_p is the peak emission rate. Likewise, the bottom panel shows the night time OH volume emission rate (on 20 June 2005). Please note that, the x-axis scales are different due to the day and night time VER variations.

3. Results and discussion

3.1. Climatology of seasonal variation of OH PER, temperature and ozone volume mixing rate (VMR)

To characterize the seasonal variation of OH emission layer, the top panel of Fig. 2 shows the composite (constructed from 13 years of monthly averaged data) monthly variation of SABER 1.6 μm OH emission data in the heights of 75–105 km. In this figure, while the left panel shows the variation during daytime, the right panel shows it during nighttime. It may be noted that the day and night time scales are different as the emission rates are quite different for day and night times. Similarly, the middle panel shows the temperature and the bottom panel shows the the O_3 volume mixing ratio (VMR) (day and night time scale s are different as the VMR is quite different for day and night times).